Calculations of the minimal perimeter for N deformable cells of equal area confined in a circle

S.J. Cox
Institute of Mathematical and Physical Sciences,
University of Wales Aberystwyth, Ceredigion SY23 3BZ, UK

July 17, 2006

Abstract

Candidates to the least perimeter partition of a disk into N planar connected regions are calculated for $N \leq 43$. A Voronoi construction is used to randomly create the candidates and then the perimeter of each is found with the Surface Evolver. Formulae for the perimeter and number of peripheral regions are given, and the candidates classified according to their topology. The simulation technique also provides improved candidates to the unconstrained problem of finding the least perimeter arrangement of N planar regions.

1 Introduction

The surface energy of a two-dimensional foam is simply its perimeter multiplied by surface tension [1]. A foam attains a local minimum of this perimeter, subject to the constraint of fixed bubble volumes. Here, we seek the two-dimensional arrangement of bubbles that gives the global minimum.

Hales [2] proved the honeycomb conjecture: that the honeycomb is the least perimeter division of the (infinite) plane into cells (bubbles) of equal area A. Each cell has six edges of length L, with A and L related by $A = 3\sqrt{3}L^2/2$. Since each edge is shared between two cells, each cell contributes a perimeter of $3L$. Thus the total perimeter is $E_{hex} = 3NL$, where N is the number of cells.

For finite collections of cells, there are proofs (see [3]) that a circle provides the least perimeter of a single cell, the familiar double bubble is the least perimeter arrangement of two cells, and that the "obvious" candidate for $N = 3$ is optimal [4]. For $N > 3$, estimates of the optimal configuration and the associated perimeter have been given for $N \leq 15$ [5, 6], and extended to $N \leq 22$ [7], and then N up to 42 [8]. The candidates show, in general, a more or less rounded overall shape with mostly hexagonal cells in the centre (see figure 1a).

Perimeter bounds for the finite case have been given by Heppes and Morgan [9]. These are asymptotically of the form

$$E/L = 3N + k\sqrt{N}, \tag{1}$$

for some number k. The first term is the usual contribution of hexagonal cells and the $\sqrt{N}$ term is a correction due to the peripheral cells. In fitting this form to the results of simulations, the second term must also account for deviations of hexagons from regularity and any non-hexagonal cells in the centre, or bulk, of the cluster.

Simulations by Cox and Graner [10] showed that for N up to 10,000 the trade-off between reducing the length of the periphery of the cluster and attaining regular hexagons in the bulk is "won" by the bulk. That is, the perimeter E of the cluster is minimized by a cluster that has a periphery that is itself hexagonal, allowing the bulk to consist only of regular hexagons, rather than rounding the cluster to reduce the length of the periphery.

In this paper we impose the periphery of the cluster to be circular, determine candidates to the least perimeter arrangement, and examine the influence of the periphery in creating deviations of the cluster from the regular hexagonal lattice. That is, we seek the least perimeter partition of a circular disk into N cells of equal area, equivalent to the energetic groundstate for N monodisperse bubbles or the optimal packing of equal-area objects in a disk. We assume that each cell is *connected*, that is, it is not split into a number of components. This seems reasonable, but remains unproven for $N > 3$; indeed, it is one of the main stumbling blocks to proving that a given candidate is optimal. We examine values of N up to 43 (beyond which the simulation technique performs less well since there are many more possible topologies to explore) and record the least perimeter, the number of peripheral cells N_p and the topology (number of sides) of the cells in the bulk of the cluster.

Topological defects are classified using the idea of *charge* [11]. Bulk cells have a charge $q = 6 - n$, where n is the number of sides. Thus hexagons have zero charge. In the same way, peripheral cells have charge $q = 5 - n$. The total charge of the cluster is then $\sum q = 6$. In the free cluster case, positive and negative charges tend to be associated, and the remaining positive charges are usually well-spaced around the periphery of the cluster [8].

The aim of this paper is partly to inspire the derivation of exact results, as in the recent work of Cañete and Ritore [12] for $N = 3$. Tomonaga [13] assumed connectedness, and explored candidate solutions for $N = 2$ to 5 and Bleicher [14] gave conjectured minimizers for $N \leq 6$, although neither found the optimal candidate for $N = 5$ and 6: improved estimates can be found in [12] and agree with the present study.

In addition, in the same way that the minimal arrangement of a free cluster of cells appears to predict the arrangement of retinal cells in *Drosophila* [15], the solutions found here may provide information about other biological structures, such as the arrangement of seeds in a flower [16, 17].

The structure of perimeter-minimizing bubble clusters is at least locally well defined [14]. Perimeter minimization implies Plateau's rules [18]: three and only three edges meet at a point at 120° [19]. The Laplace Law relating pressure difference and curvatures gives the further condition that each edge is a circular arc. These conditions are augmented in the present case by the rule that edges meet the bounding circular wall at 90°. Topological relationships between peripheral and bulk cells in a confined two-dimensional foam are derived in [20] in the context of diffusion-driven coarsening.

2 Method

The value of surface tension, which is equal for all internal edges, is taken as one. Candidates to the minimal arrangement of cells are created as follows. 250 points are scattered at random in a unit square and their Voronoi partition calculated. Peripheral Voronoi cells are successively removed until N cells remain in the centre of the domain. This structure is imported into the Surface Evolver [21], which we use in circular arc mode. The cell areas are set to the value $A = 3\sqrt{3}/2$ and the tension of peripheral edges is set to 10^2 to approximate the circular constraint. (This level of description is sufficient to distinguish the least perimeter candidate.) The equilibrium perimeter E of the candidate configuration is then calculated, excluding the contribution of the outer wall of length $E_w/L = 2\sqrt{\pi NA}$, allowing T1 neighbour switching events to occur when short edges

result. Up to 25 successive attempts at finding a lower perimeter structure "close" to this one are performed by initiating a T1 event on the shortest edge in the cluster and calculating the new equilibrium.

This complete procedure is repeated up to two thousand times for each N, and the least-perimeter candidate recorded in each case. Finally, an exact circular constraint is imposed upon this candidate and the perimeter recorded precisely.

We find this method to be an improvement on the one used by Cox et al. [8]. In that work candidates were generated from a starting topology consisting of hexagons. In each "shuffling" step the cluster was randomly perturbed and a new configuration created by performing a T1 change on the shortest edge. A method of this kind evolves very slowly since only local changes are made in each step, and the algorithm easily becomes stuck in a local minimum. With the present method, we introduce a a balance between this type of shuffling step and starting again from a new, randomly generated, structure, albeit one without hexagonal structure. This allows a wider exploration of possible candidates, with improved results as discussed below.

3 Simulation results

Candidates to the minimum perimeter partition of a disk into N regions of area $A = 3\sqrt{3}/2$ are shown in figures 2 and 3 and recorded in Table 1. The values of conjectured optimal perimeter and the corresponding number of peripheral cells are shown in figure 4.

The perimeter increases monotonically with N. A fit of equation (1) to the perimeter has $k = -2.336 \pm 0.158$. The addition of the peripheral term E_w gives a value of $k = 3.378$, slightly greater than the asymptotic value of 3.097 for free clusters [8, 9], indicating that the cells are more deformed in this constrained case.

The number of peripheral cells N_p does not increase monotonically, although, as for the free case, it scales roughly as $\sqrt{N}$ [8]. A fit to the form $N_p = -3 + k_p\sqrt{N}$ has $k_p = 3.407 \pm 0.459$.

Turning now to the actual configuration of cells, we note a number of symmetric patterns. The defect-free cases of $N = 7, 19, 37, \ldots, 1 + 3i(i+1), i \in \mathbb{N}$, have a 6-fold, rotationally symmetric, structure consisting of nested rings of hexagons.

Similarly, some configurations attain rotational symmetry by having a single defect at the very centre of the cluster and hexagons elsewhere in the bulk. Five-fold rotational symmetry is exhibited for $N = 6, 16, 31$, and may continue to be found for N of the form $1 + 5i(i+1)/2, i \in \mathbb{N}$. Seven-fold symmetry is found for $N = 8$ and 22, but surprisingly does not hold for $N = 43$, the next in the series (this symmetric cluster has $E/L = 114.006688$, 0.2% greater than the best candidate).

Of the other candidates, all of those for $N \leq 24$ show reflective symmetry as do $N = 27, 43$ and all even N in the range $30 \leq N \leq 40$.

It is therefore clear that the least perimeter structure does not always have only hexagons in the bulk, although in addition to the six-fold rotationally symmetric cases above, $N = 10, 12, 14, 24, 27, 30$ and 40 do. Figure 1 emphasises that this is not because such candidates were not checked for each N. Instead, in many cases the perimeter is reduced below that of the hexagonal candidate with a five- or seven-sided defect in the bulk of the cluster. Seven-sided cells usually neighboured by at least one five-sided cell, and no more than one seven-sided cell is ever present.

How do the candidates compare with those for the free cluster problem? The configurations found in [8], despite being rounded at low N, do not all show the same topology as the candidates found here. We make a comparison by relaxing the boundary constraint from each candidate in figures 2 and 3, to give a free cluster with the same topology, as in figure 1d). The difference in perimeter between these and the candidates found in [8] is shown in figure 5. In most cases this difference is zero, indicating that the same topology solves both the least perimeter partition of the

N	E/L	N_p	Bulk topology
2^*	2.572148	2	
3^*	4.725338	3	
4	7.176379	4	
5	9.829442	5	
6	12.043888	5	5_1
7	14.436146	6	6_1
8	17.097664	7	7_1
9	19.956447	7	$5_1 6_1$
10	22.537405	8	6_2
11	25.150735	8	$5_1 6_2$
12	27.721101	9	6_3
13	30.503419	9	$5_1 6_3$
14	33.167561	10	6_4
15	35.963480	10	$5_2 6_2 7_1$
16	38.559205	10	$5_1 6_5$
17	41.292347	11	$5_1 6_4 7_1$
18	43.910651	11	$5_1 6_6$
19	46.484518	12	6_7
20	49.468519	13	$6_6 7_1$
21	52.206625	13	$5_1 6_6 7_1$
22	55.016341	14	$6_7 7_1$

N	E/L	N_p	Bulk topology
23	57.842433	13	$5_1 6_9$
24	60.544438	14	6_{10}
25	63.359499	14	$5_1 6_9 7_1$
26	66.089961	14	$5_1 6_{11}$
27	68.757748	15	6_{12}
28	71.723683	15	$5_1 6_{11} 7_1$
29	74.485437	15	$5_1 6_{13}$
30	77.216169	16	6_{14}
31	80.149221	15	$5_1 6_{15}$
32	82.934537	16	$5_1 6_{14} 7_1$
33	85.689991	16	$5_2 6_{14} 7_1$
34	88.486652	17	$5_1 6_{15} 7_1$
35	91.207126	17	$5_1 6_{16} 7_1$
36	93.888640	17	$5_1 6_{18}$
37	96.587085	18	6_{19}
38	99.639955	19	$6_{18} 7_1$
39	102.529436	19	$5_1 6_{18} 7_1$
40	105.492341	19	6_{21}
41	108.271113	19	$5_1 6_{20} 7_1$
42	111.149408	18	$5_2 6_{22}$
43	113.851517	19	$5_1 6_{23}$

Table 1: Perimeter E/L, the number N_p of peripheral cells and the bulk topology of the minimal candidates found here. The topology is recorded in the form $5_l 6_m 7_n$, indicating l 5-sided internal cells, m 6-sided internal cells etc. Note that the topology of the periphery can be inferred from this: the number of 4-sided cells on the periphery is $6-l+n$, the remainder are 5-sided. Asterisked values were calculated analytically.

disk and the least perimeter free arrangement of cells. Positive differences indicate that the least perimeter for a cluster constrained within a circular boundary is found by changing the topology. In four cases, $N = 23, 29, 35$ and 41 we find improved candidates to the free cluster problem; these are shown in figure 6.

4 Conclusion

We have found candidates to the minimal perimeter of partitions of a circular disk into N regions of equal area. Equivalently, we have found the global energetic groundstate of a two-dimensional foam confined within a circular boundary. This extends previous work on finite, unbounded, clusters.

The perimeter of the minimal candidates is well-described by the formula $E/L = 3N - 2.336\sqrt{N}$ and the number of peripheral cells by $N_p = -3 + 3.407\sqrt{N}$. Thus the "excess" perimeter $E/L - 3N$ scales linearly with N_p.

Classifying the structures found by their symmetry is an attractive concept but, as the optimal solution for $N = 43$ shows, frustrating. Few general results emerge from the data, except that only five, six and seven-sided cells are observed. In only one instance ($N = 22$) is a seven-sided cell not adjacent to a five-sided one. Even the defect-free values of N of the form $1 + 3i(i+1), i \in \mathbb{N}$ will not be perimeter-minimising at large N since their overall hexagonal shape will be penalised and improved upon by rounding the corners, as figure 7 shows.

The simulation technique used here is an improvement on previous attempts [8], as indicated by the new candidates proposed for the free cluster problem. However, for each N, the algorithm, even though repeated thousands of times, explores only a few hundred different candidates at most. It remains an open question as to how many candidates actually exist, but it is surely many more than this for the largest values of N treated here. To extend such a search to larger N would therefore require a more sophisticated numerical procedure.

Finally, related problems include the problems of finding the least perimeter partition of a triangle [14] and a square [13, 14]. This presents an interesting area of further study, and one in which numerical solutions such as those presented here may be usefully applied.

Acknowledgements

The author thanks K. Brakke, not only for his provision of the Surface Evolver software and advice on its use, but for supplying a Voronoi code with Evolver output. The work was stimulated by discussions with T. Tarnai and improved by discussions with F. Graner, A. Cañete and F. Morgan.

References

[1] D. Weaire and S. Hutzler. 1999 *The Physics of Foams*. Clarendon Press, Oxford.

[2] T.C. Hales. 2001 The honeycomb conjecture. *Discrete Comput. Geom.* **25**:1–22.

[3] F. Morgan. 2000 *Geometric Measure Theory: A Beginner's Guide*. Academic Press, San Diego. 3rd edition.

[4] W. Wichiramala. 2004 Proof of the planar triple bubble conjecture. *J. reine. angew. Math.* **567**:1–50.

[5] M. Alfaro, J. Brock, J. Foisy, N. Hodges and J. Zimba. 1990. Compound soap bubbles in the plane, SMALL Geometry Group report.

[6] F. Morgan. 1994 Mathematicians, including undergraduates, look at soap bubbles. *Amer. Math. Monthly* **101**:343–351.

[7] M.F. Vaz and M.A. Fortes. 2001 Two-dimensional clusters of identical bubbles. *J. Phys.: Condens. Matt.* **13**:1395–1411.

[8] S.J. Cox, F. Graner, M.F. Vaz, C. Monnereau-Pittet and N. Pittet. 2003 Minimal perimeter for N identical bubbles in two Dimensions: calculations and simulations. *Phil. Mag.* **83**: 1393–1406.

[9] A. Heppes and F. Morgan. 2005 Planar Clusters and Perimeter Bounds . *Phil. Mag.* **85**: 1333–1345.

[10] S.J. Cox and F. Graner. 2003 Large two-dimensional clusters of equal-area bubbles. *Phil. Mag.* **83**:2573–2584.

[11] F. Graner, Y. Jiang, E. Janiaud and C. Flament. 2001 Equilibrium states and ground state of two-dimensional fluid foams. *Phys. Rev. E* **63**:011402.

[12] A. Cañete and M. Ritore. 2004 Least-perimeter partitions of the disk into three regions of given areas. *Indiana Univ. Math. J.* **53**:883–904.

[13] Y. Tomonaga. 1974 *Geometry of Length and Area*. Dept. of Mathematics, Utsunomiya University, Japan.

[14] M.N. Bleicher. 1987 Isoperimetric divisions into several cells with natural boundary. In *Intuitive geometry*. North-Holland, Amsterdam. Colloq. Math. Soc. János Bolyai, **48**:63–84.

[15] T. Hayashi and R.W. Carthew. 2004 Surface mechanics mediate pattern formation in the developing retina. *Nature* **431**:647–652.

[16] T. Tarnai. 2002 Optimum packing of circles in a circle. In I. Hargittai and T. Laurent (eds), *Symmetry 2000*. Portland pp. 121–132.

[17] T. Tarnai and K. Miyazaki. 2003 Circle Packings and the Sacred Lotus. *Leonardo* **36**:145–150.

[18] J.E. Taylor. 1976 The structure of singularities in soap-bubble-like and soap-film-like minimal surfaces. *Ann. Math.* **103**:489–539.

[19] J.A.F. Plateau. 1873 *Statique Expérimentale et Théorique des Liquides Soumis aux Seules Forces Moléculaires*. Gauthier-Villars, Paris.

[20] M. Emília Rosa and M.A. Fortes. 1999 Coarsening of two-dimensional foams confined by walls. *Phil. Mag. A* **79**:1871–1886.

[21] K. Brakke. 1992 The Surface Evolver. *Exp. Math.* **1**:141–165.

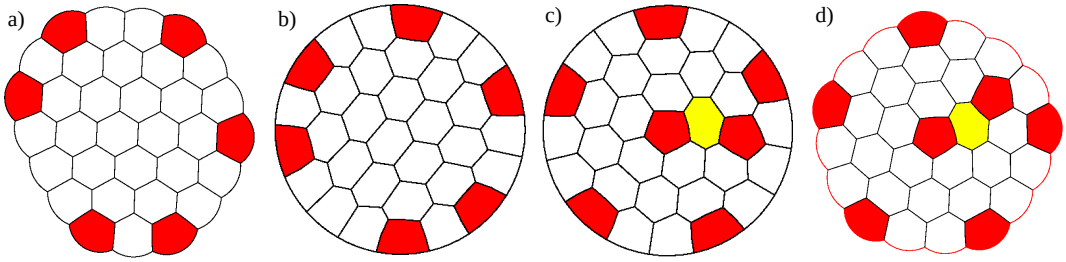

Figure 1: Free and constrained candidates for $N = 33$. Cells with charge $q = +1$ are coloured red, those with charge -1 are yellow. (a) The least perimeter free cluster found in [8], with perimeter $E/L = 116.582537$. (b) The cluster in (a) confined within a circle, with bulk topology 6_{16} and perimeter $E/L = 85.805016$. (c) The least perimeter cluster obtained, with $E/L = 85.689991$ and bulk topology $5_2 6_{14} 7_1$. Thus a bulk honeycomb structure within a disk is not always optimal. (d) The least perimeter partition of the disk, from (c), with the boundary relaxed to provide a candidate to the free cluster problem, in this case with greater perimeter $E/L = 116.793811$.

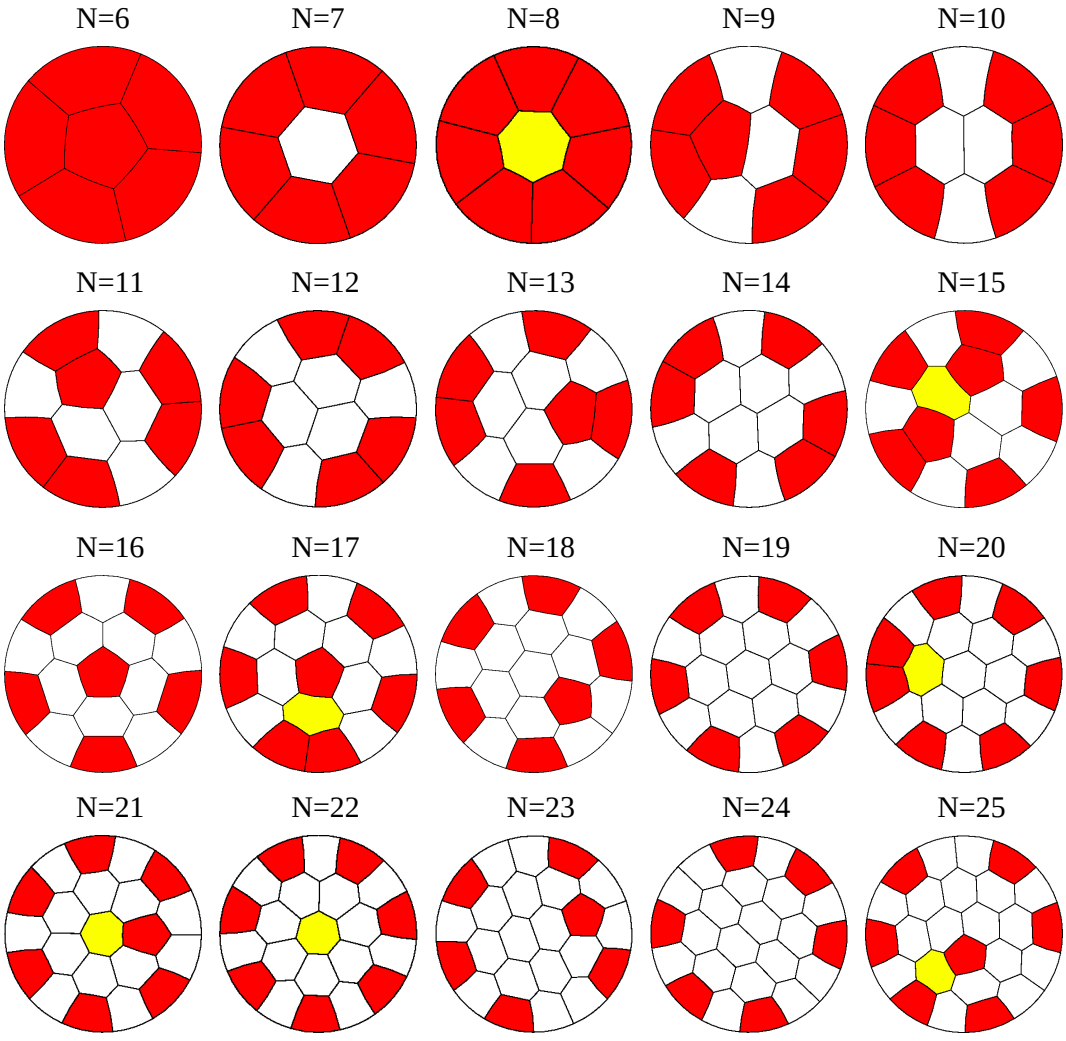

Figure 2: Candidate configurations for the least-perimeter partition of the disk into N regions of equal area for $6 \leq N \leq 25$.

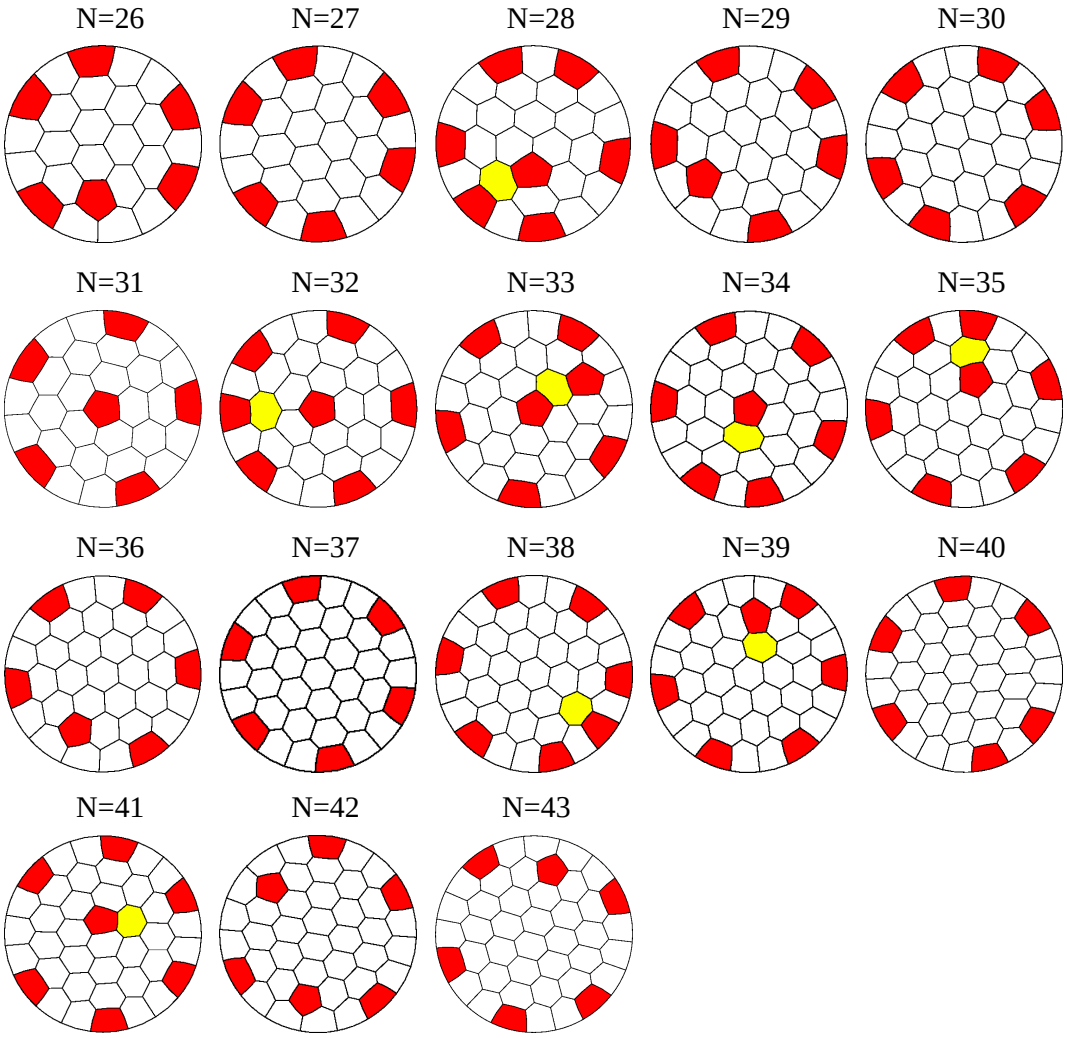

Figure 3: Candidate configurations for the least-perimeter partition of the disk into N regions of equal area for $26 \leq N \leq 43$.

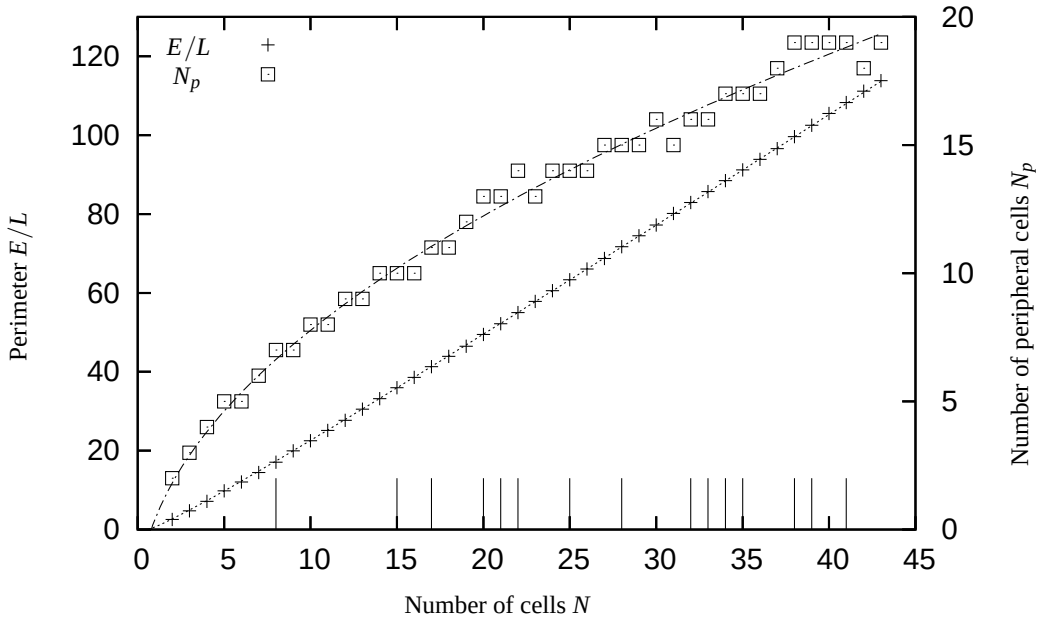

Figure 4: The perimeter E/L and number N_p of peripheral cells of the candidate configurations shown in figures 2 and 3. Lines are best fits to the forms given in the text. The short vertical lines indicate those configurations that have a single negative charge.

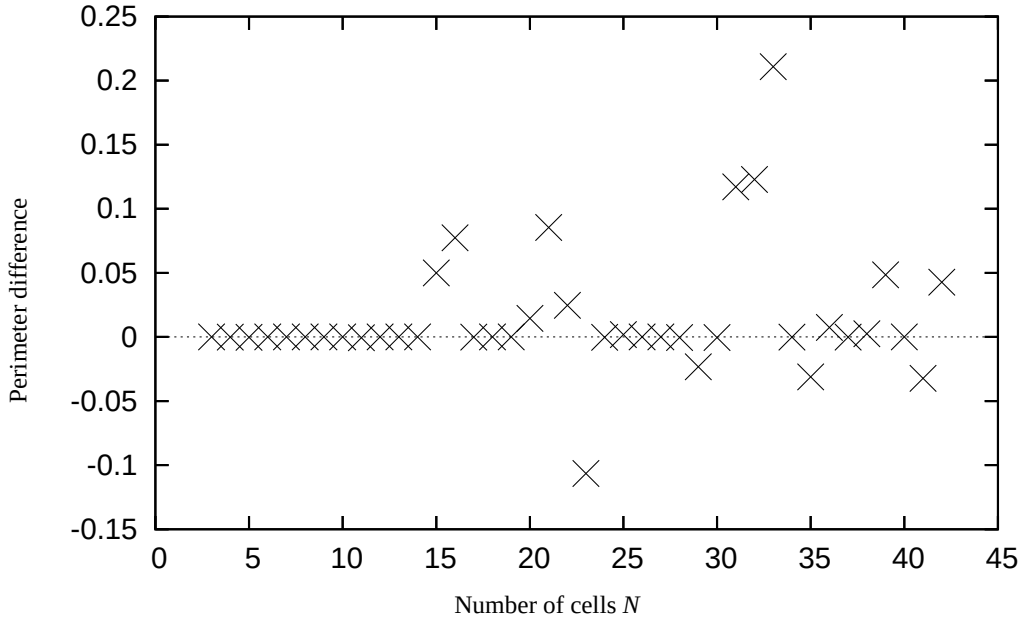

Figure 5: Least perimeter candidates for free clusters are constructed by relaxing the boundary of the confined clusters in figures 2 and 3. Here, we compare their perimeter with the candidates found in [8]. In just over half of the cases the clusters are the same, and several more of the topologies dictated by the circular constraint have greater perimeter when unrestrained. The candidate for $N = 33$, illustrated in figure 1c) and d), shows the greatest difference. Negative differences indicate that four better candidates to the free cluster problem are found, for $N = 23, 29, 35$ and 41.

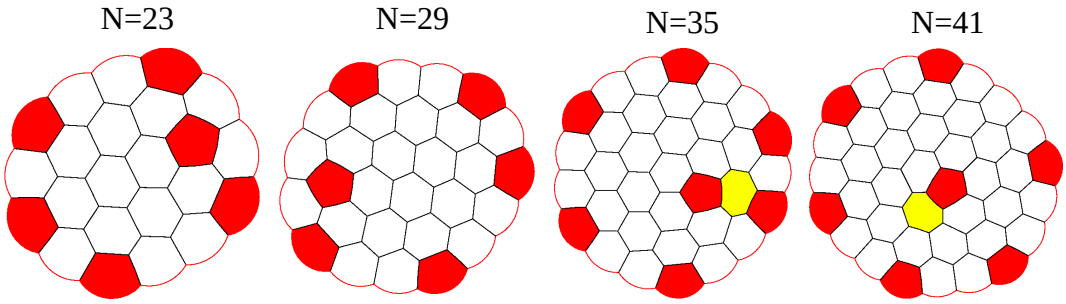

Figure 6: Improved candidates (cf. [8]) to the free cluster problem for $N = 23, 29, 35$ and 41 arise from the confined problem considered here.

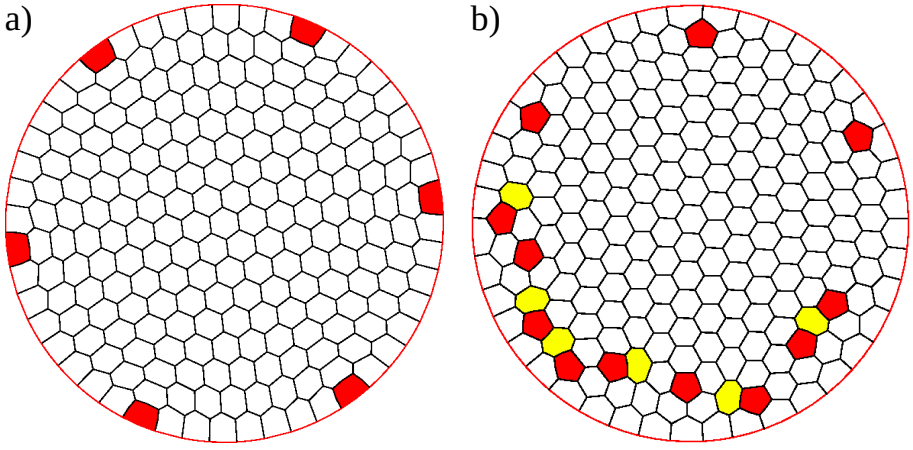

Figure 7: For larger N, nested rings of hexagons are no longer the least perimeter partition of the disk. (a) For $N = 217$, with $i = 8$ shells of cells, the perimeter is $E/L = 618.636583$. (b) Despite having many more defects, this cluster of 217 cells, although undoubtedly not optimal, has perimeter $E/L = 618.531445$.